

# Efficient statistical classification of satellite measurements

PETER MILLS\*\*

February 5, 2016

## Abstract

Supervised statistical classification is a vital tool for satellite image processing. It is useful not only when a discrete result, such as feature extraction or surface type, is required, but also for continuum retrievals by dividing the quantity of interest into discrete ranges. Because of the high resolution of modern satellite instruments and because of the requirement for real-time processing, any algorithm has to be fast to be useful. Here we describe an algorithm based on kernel estimation called Adaptive Gaussian Filtering that incorporates several innovations to produce superior efficiency as compared to three other popular methods:  $k$ -nearest-neighbour (KNN), Learning Vector Quantization (LVQ) and Support Vector Machines (SVM). This efficiency is gained with no compromises: accuracy is maintained, while estimates of the conditional probabilities are returned. These are useful not only to gauge the accuracy of an estimate in the absence of its true value, but also to re-calibrate a retrieved image and as a proxy for a discretized continuum variable. The algorithm is demonstrated and compared with the other three on a pair of synthetic test classes and to map the waterways of the Netherlands. Software may be found at: <http://libagf.sourceforge.net>.

## 1 Introduction

Remote-sensing satellite instruments are returning increasing amounts of information about the Earth's surface and atmospheric state. To be useful,

---

\*\*Corresponding author: [petey@peteysoft.org](mailto:petey@peteysoft.org) 1-613-833-3022

these data need to be processed to retrieve the quantities of interest, ideally in real time or better. Surface-detecting instruments, such as Landsat, MODIS and AVHRR in the visible and infra-red and AMSR-E and SSM/I in the microwave, are vital tools for mapping the globe, especially when it is constantly shifting as in the case of sea ice (Spreen *et al.*, 2008). Statistical classification can help determine what the instrument is “seeing,” whether that be crops, water, road or ice, underneath a given pixel or from a combination of pixels; for instance, picking out crops of a particular type in a Landsat image (Laue, 2004). This type of study can be useful both for producing maps and gathering statistics. Even when a discrete type is not required, statistical classification can still be useful for continuum retrieval and inversion by dividing the quantity of interest into discrete ranges (Mills, 2009).

In supervised statistical classification, we are interested in determining the class,  $c$  of a test vector,  $\vec{x}$ , based on a series of known input:output relations,  $\{\vec{x}_i : c_i\}$ , also known as training data. The vector,  $\vec{x}$ , could correspond to a measurement vector, i.e. counts from several channels of one or more satellite instruments, while the class,  $c$  might correspond to a surface type, e.g. crops, forest, field, road, water, etc. The class is related to the inputs via a conditional probability,  $P(j|\vec{x})$ , which is discretely represented by the training data. Normally, we seek the the most likely class (maximum likelihood estimation):

$$c = \arg \max_j P(j|\vec{x}) \quad (1)$$

thus we need some method of estimating the conditional probabilities. This is the function of a kernel-density estimator (Terrell and Scott, 1992) and of a  $k$ -nearest-neighbours (KNN) method (Michie *et al.*, 1994). Other methods, such as Learning Vector Quantisation (LVQ) (Kohonen, 2000) and Support Vector Machines (SVM) (Müller *et al.*, 2001) skip this step in favour of directly determining the class domains. Note that kernel estimation should not be confused with methods based on the “kernel trick” such as SVM, described in section 4.2.3.

Because of the large amount of data involved and the necessity for real-time processing, an important feature of modern satellite inversion algorithms, including statistical classification, is speed. In Mills (2009), a method for statistical classification called “Adaptive Gaussian Filtering” (AGF), based on kernel estimation, was briefly described and applied to Advanced Microwave Sounding Unit (AMSU) data to discretely retrieve water vapour in

the upper troposphere. Because this retrieval required several days of AMSU swath data, comprising tens of millions of individual measurements, the classification algorithm had to be fast. Here we describe the algorithm more completely and demonstrate its superior performance compared to three other popular methods by first applying them to an artificial test case and then using them to classify surface types in Landsat images.

The AGF algorithm incorporates several critical innovations that make it extremely efficient without sacrificing accuracy or the ability to estimate the conditional probabilities. These are needed to set a definite confidence on the accuracy of an estimate in absence of knowledge of its true value. The following refinements are applied to a variable-bandwidth, kernel density “balloon” estimator (Terrell and Scott, 1992) based on Gaussian kernels. First, the filter width is matched to the sample density using the properties of the exponential function, avoiding unnecessary computation of exponentials (section 3.1). Second, calculations are restricted to a set of  $k$ -nearest-neighbours found in  $n \log k$  time with a binary tree (section 3.2). Third, because probability estimates are continuous, a pre-trained model can be generated by searching for the class-borders with guaranteed, super-linear convergence (sections 2.2 and 3.3). Fourth, using the pre-trained model, the conditional probabilities are interpolated from gradients at the class-border (section 2.3).

## 2 Essential description of the algorithm

### 2.1 Adaptive Gaussian filtering

The  $k$ -nearest-neighbours (KNN) is a well-known and effective technique of estimating probability densities and performing classifications. It works by picking from the training data the  $k$  samples nearest the test point and determining the class by voting (Michie *et al.*, 1994). A simple refinement to this method would be to weight the samples according to distance as in a simple linear filter. Given a set of points,  $\{\vec{x}_i\}$ , the probability density function (PDF) of a test point,  $\vec{x}$ , may be estimated as follows:

$$P(\vec{x}) \approx \frac{W}{nN} \quad (2)$$

$$W = \sum_{i=0}^n w_i \quad (3)$$

where  $w_i$  is the weight of the  $i$ th sample,  $n$  is the number of samples and  $N$  is a normalisation coefficient. Its justification is a Monte Carlo integration with importance sampling (Press *et al.*, 1992), except that here we solve for the importance distribution by multiplying it with a peaked, but otherwise essentially arbitrary function, and assume that it is roughly constant.

The magnitude of the weights must decrease with distance and in the isotropic case they are given by:

$$w_i = f(d_i) \quad (4)$$

$$d_i = |\vec{x} - \vec{x}_i| \quad (5)$$

where  $f$  is a filter function and  $d_i$  is the distance of the  $i$ th sample from the test point. The upright brackets denote a metric, typically Cartesian, although in theory any metric could be used. In practise, it is often simplest and most efficient to first re-scale or otherwise transform the variables so that a Cartesian metric is then appropriate. The normalisation coefficient will be given by:

$$N = \int_A f(|\vec{x} - \vec{y}|) d\vec{y} \quad (6)$$

where  $A$  is the domain of the samples. This technique is known as a fixed-bandwidth kernel-density estimator (Terrell and Scott, 1992).

A natural choice for  $f$  would be a Gaussian:

$$f(r) = \exp\left(-\frac{r^2}{2\sigma^2}\right) \quad (7)$$

where  $\sigma$  is the filter width and  $N = (2\pi)^{D/2}\sigma^D$  with  $D$  as the number of dimensions. Using a fixed filter width may mean that in regions of low density, all samples will fall in the tails of the filter with very low weighting, while regions of high density will find an excessive number of samples in the central region with weighting close to unity. Thus we vary the filter width according to density so that an optimal number of samples falls within the central region.

According to the definition of the probability density, the local average point spacing will be given as follows:

$$\delta = \frac{1}{[nP(\vec{x})]^{1/D}} \quad (8)$$

We wish to vary the filter width so that it matches the point spacing:

$$\sigma^{(opt)} = k_1 \delta = \frac{k_1}{[nP(\vec{x})]^{1/D}} \quad (9)$$

where  $k_1$  is a coefficient. Substituting the approximated PDF from (2) through (7) produces the following that must be solved for  $\sigma^{(opt)}$ :

$$W(\sigma^{(opt)}) \approx k_1^D (2\pi)^{D/2} = \text{const.} \quad (10)$$

Thus, correctly selecting a fixed value for  $W$  (call it  $W_c$ ) in (3) should produce an “optimal” (as we have defined it) filter width. The proof is valid for all functions for which  $N \propto \sigma^D$  which is true for all functions of the form  $f(r/\sigma)$  for which the integral in (6) exists.

The quantity  $W_c$  may be thought of as roughly equivalent to  $k$  in a KNN scheme. Here we have created what is known as a variable-bandwidth kernel-density “balloon” estimator: variable-bandwidth means that the filter width is varied depending on the location in the sample space, while “balloon” means that it is varied based on the location of the test point, not the training samples (as in a “pointwise estimator”), thus for a given estimate the same filter width is applied to all training samples (Terrell and Scott, 1992).

To use the method for classification, we first estimate the conditional probability as follows:

$$P(m|\vec{x}) \approx \frac{1}{W} \sum_{i,c_i=m} w_i \quad (11)$$

where  $c_i$  is the class associated with the  $i$ th sample.

## 2.2 Finding the class borders

The chief advantage of this scheme over a KNN is that it produces results that are both continuous and differentiable. Both properties are desirable in that they allow us to search for a unique border between the classes (discrimination border) and hence make more rapid classifications. Assuming that there are only two classes, the difference in their conditional probabilities is:

$$R(\vec{x}) = P(2|\vec{x}) - P(1|\vec{x}) \approx \frac{1}{W} \sum_i (2c_i - 3)w_i \quad (12)$$

where 1 and 2 are the classes and  $c_i$  is the class of the  $i$ th sample. The borders are found by setting this expression to zero,  $R(\vec{x}) = 0$ . With an adaptive Gaussian filter, the derivative becomes: <sup>1</sup>

$$\frac{\partial R}{\partial x_j} \approx \frac{1}{\sigma^2 W_c} \sum_i w_i (2c_i - 3) \left[ x_{ij} - x_j - d_i^2 \frac{\sum_k w_k (x_{kj} - x_k)}{\sum_k d_k^2 w_k} \right] \quad (13)$$

where  $x_{ij}$  is the  $j$ th coordinate of the  $i$ th sample, while  $x_j$  is the  $j$ th coordinate of the test point. Derivatives will be necessary both for estimating the class of the test point (see below) and then extrapolating the conditional probabilities (section 2.3) as well as useful (though not essential) for searching out the discrimination border (section 3.3).

The border may be sampled as many times as necessary, giving a set of vectors,  $\{\vec{b}_i\}$ , along with their corresponding gradients,  $\{\nabla_{\vec{x}} R|_{\vec{x}=\vec{b}_i}\}$ . The class of a test point,  $\vec{x}$ , is calculated as follows:

$$j = \arg \min_i |\vec{b}_i - \vec{x}| \quad (14)$$

$$p = (\vec{x} - \vec{b}_j) \cdot \nabla_{\vec{x}} R|_{\vec{x}=\vec{b}_j} \quad (15)$$

$$c = (3 + p/|p|)/2 \quad (16)$$

where  $c$  is the class. The specific procedure used to sample the class border will be described in section 3.3.

Note that it is easy to generalise a two-class classification to multiple classes, although the best method of doing so will be highly problem-dependent.

## 2.3 Extrapolating the conditional probabilities

The value of  $R$  may be extrapolated to the test point. Consider a pair of one-dimensional classes composed of two equal-sized Gaussians of width  $s$  separated by a distance  $2a$  with the class border lying at  $b$ . Let  $\tilde{R}$  be the difference between the conditional probabilities:

$$\tilde{R}(x) = P(2|x) - P(1|x) \quad (17)$$

$$= \frac{P(2, x) - P(1, x)}{P(1, x) + P(2, x)} \quad (18)$$

$$= \frac{e^{-\frac{(x-b+a)^2}{2s^2}} - e^{-\frac{(x-b-a)^2}{2s^2}}}{e^{-\frac{(x-b+a)^2}{2s^2}} + e^{-\frac{(x-b-a)^2}{2s^2}}} \quad (19)$$

<sup>1</sup>Superscripts have been omitted. For a derivation of this equation (which does not appear in the original paper) please refer to Appendix A.

Simplifying:

$$\tilde{R}(x) = \tanh\left(\frac{a(x-b)}{s^2}\right) \quad (20)$$

To approximate the difference in conditional probabilities,  $R(x)$ , between an arbitrary pair of (well-behaved) 1-D classes, we fit  $\tilde{R}(x)$  to  $R(x)$  by setting:

$$\tilde{R}(b) = R(b) = 0 \quad (21)$$

$$\left.\frac{d\tilde{R}}{dx}\right|_{x=b} = \frac{a}{s^2} = \left.\frac{dR}{dx}\right|_{x=b} \quad (22)$$

We can approximate  $R$  for a pair of multi-dimensional classes in the same way:

$$R(\vec{x}) \approx \tilde{R}(\vec{x}) \equiv \tanh p \quad (23)$$

It is easy to show:

$$\tilde{R}(\vec{b}_j) = 0 \quad (24)$$

$$\nabla_{\vec{x}}\tilde{R}|_{\vec{x}=\vec{b}_j} = \nabla_{\vec{x}}R|_{\vec{x}=\vec{b}_j} \quad (25)$$

The approximation assumes that the PDFs of the classes are roughly Gaussian near the discrimination border.

## 3 Refinements

### 3.1 Solving for the filter width

The properties of the exponential function can be used to solve for the filter width by iteratively squaring the weights. Let the  $j$ th weighting coefficient of the  $i$ th sample be given as:

$$w_i^{(j)} = \exp\left(\frac{d_i^2}{2(\sigma^{(j)})^2}\right) \quad (26)$$

where  $\sigma^{(j)}$  is the  $j$ th filter width. Each subsequent iterate is defined as the square of its previous:

$$w_i^{(j)} = \left(w_i^{(j-1)}\right)^2 \quad (27)$$

consequently the  $j$ th filter width,  $\sigma^{(j)}$ , obeys the following recursion relation:

$$\sigma^{(j)} = \frac{\sigma^{(j-1)}}{\sqrt{2}} \quad (28)$$

Following our super-scripting convention,  $W^{(j)}$  is defined as:  $W^{(j)} = \sum_i w_i^{(j)}$  with the final iteration of  $j$ , call it  $f$ , defined such that:

$$W^{(f)} \leq W_c \quad (29)$$

Obviously, the initial filter width,  $\sigma^{(0)}$ , must be chosen to be larger than the optimal, for instance by taking the total variance of the data.

The final filter width is approximated by exponential interpolation to the target total weight:

$$k_2 = \frac{\log W_c + \log W^{(f)} - 2 \log W^{(f-1)}}{2 (\log W^{(f)} - \log W^{(f-1)})} \quad (30)$$

$$\sigma^{(opt)} \approx \frac{\sigma^{(f)}}{\sqrt{k_2}} \quad (31)$$

The advantage of this scheme is that the exponentials, the most expensive part of the calculation, are computed only twice for each training sample. This is in contrast to a root-finding algorithm, which would need three computations at minimum.

### 3.2 Restricting calculations to $k$ -nearest-neighbours

Although the filter function,  $f$ , is applied in theory to all the samples, in practice only a subset of nearest neighbours will make a significant contribution to the final result. We can find  $k$  nearest neighbours in  $n \log k$  time using a binary tree. The procedure is illustrated in figure 1 and described in words in the following paragraph.

All the distance must be calculated and the  $k$  least of these will correspond to the desired neighbours. The first  $k + 1$  elements are arranged in a binary tree. The largest element will be the rightmost in the tree and must be deleted. This can be done in roughly  $\log k$  time by traversing the tree from its root. A new element is then added to the tree, also in  $\log k$  time, and the largest once again deleted. The procedure is repeated until all the elements



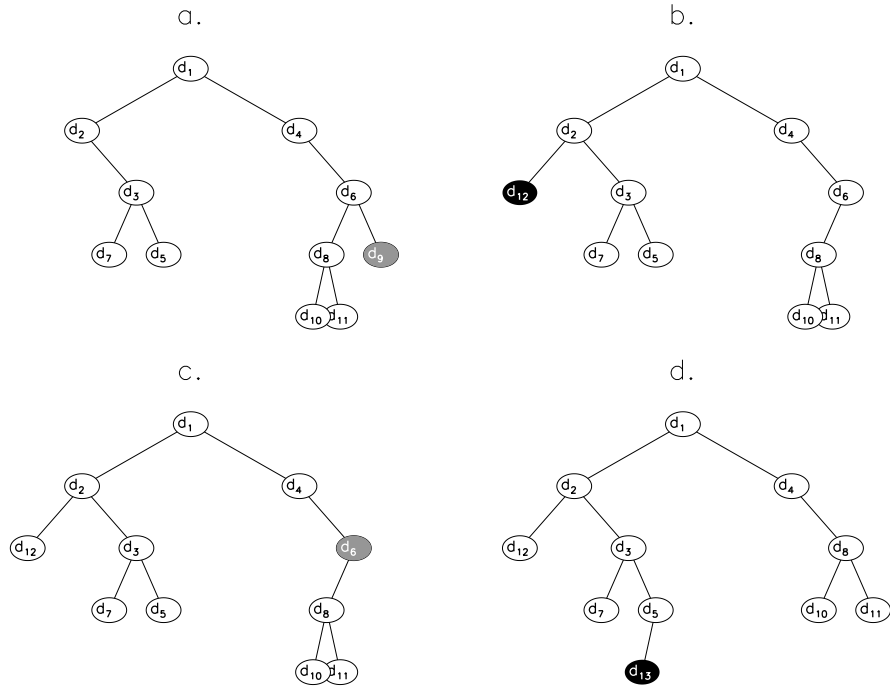


Figure 1: Demonstrating the use of a binary tree to select the 10 least elements from a list of distances,  $\{d_i\}$ . In each illustration, elements to the left are smaller, while elements to the right are larger. In (a), the tree has been filled with the first eleven members from the list and the largest element in the tree is marked for removal. In (b), the operation is completed and the 12th member from the list is added. In (c), the largest element in the tree is once again marked for removal. In (d), the operation is completed and the 13th member from the list is added.

in the list have been added to the tree and the only ones remaining are the  $k$  least (Knuth, 1998).

While it might appear that repeatedly deleting the largest element will produce an unbalanced tree, actual tests suggest that this is not the case. There are at least two mitigating factors. First, the greatest element is not always a “leaf” or lowermost element, but is itself often a node, thus an entire sub-tree will take its place as figures 1(c) and (d) exemplify. Second, new elements are constantly being added to the tree. These will tend to be larger on average than those already occupying it since we are selecting for the  $k$  least.

### 3.3 Root-finding

To sample the class border, the following procedure was employed: pick two points at random,  $\vec{x}_1$  and  $\vec{x}_2$ , belonging to classes 1 and 2 respectively. We define  $\vec{v}$  as a direction vector between the two points, e.g.:

$$\vec{v} = \vec{x}_2 - \vec{x}_1 \quad (32)$$

and solve the following for  $t$ :

$$R(\vec{x}_1 + \vec{v}t) = 0 \quad (33)$$

to find a point,  $\vec{b} = \vec{x}_1 + \vec{v}t|_{R=0}$ , randomly located on the class border.

This reduces the  $D$ -dimensional root-finding problem to only one dimension, with the root already bracketed, thus it can be found with considerable certainty. The root of a one-dimensional function is considered bracketed when we have two values of the independent variable for which the function evaluates to opposite signs, therefore at least one root must lie between (Press *et al.*, 1992). The derivatives,  $dR/dt = \nabla_{\vec{x}}R \cdot \vec{v}$ , are used as an aid to increase the speed of convergence. If both the value and the first derivative of the function are known at two locations, then it is possible to fit a unique, third-order polynomial. The root is estimated by equating the polynomial to zero, and the true root re-bracketed with this new estimate – see figure 2. The procedure is repeated until the true root is found to within a certain tolerance. This combines the fast convergence of a Newton’s method with the numerical stability of a bisection algorithm (Press *et al.*, 1992), hence we term the method, “supernewton.” The GNU scientific library (GSL) is used both to solve the cubic and to fit the function by solving the rank four linear system using Householder transformations (Galassi *et al.*, 2007).

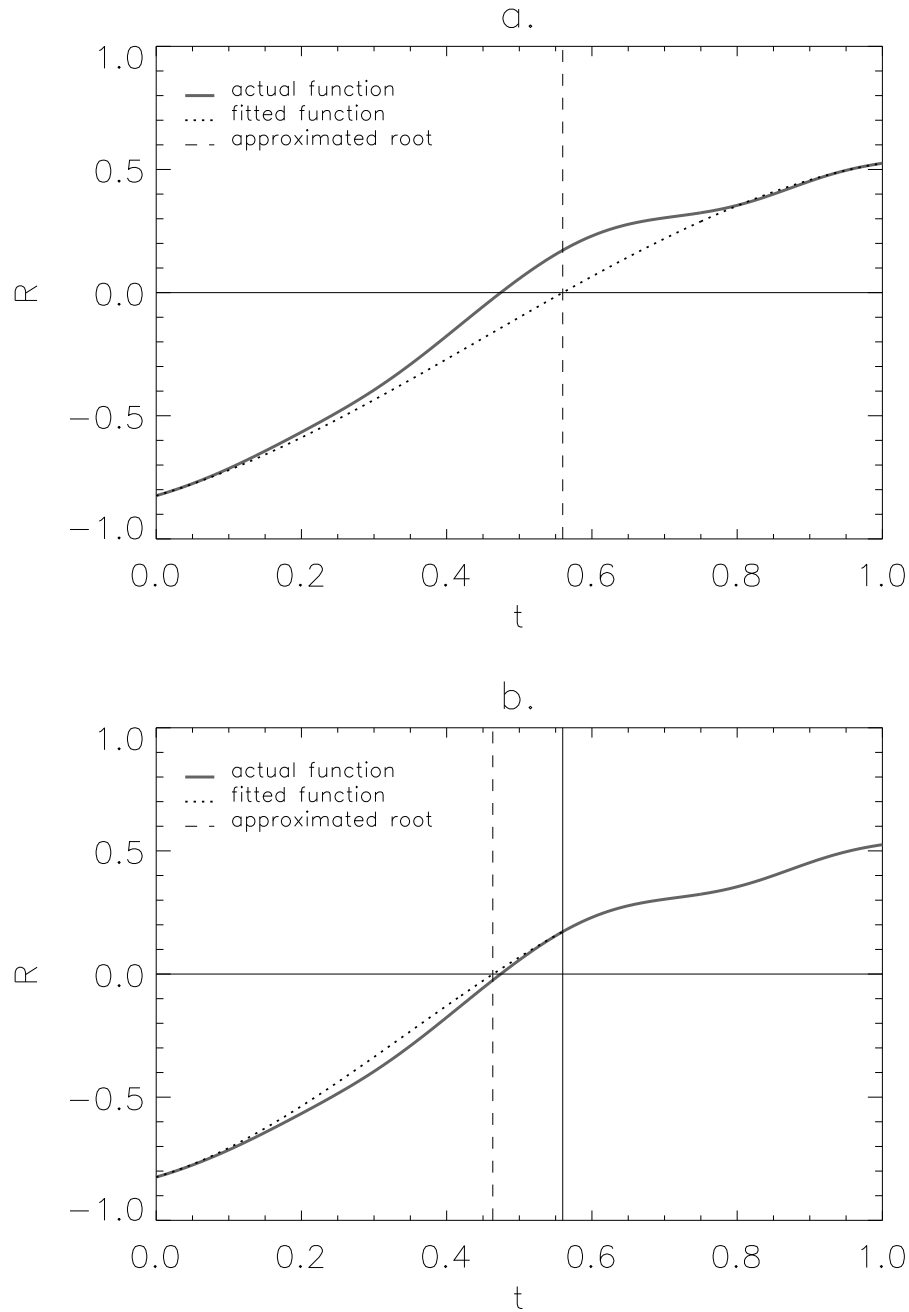


Figure 2: Demonstration of the root-finding algorithm. In a., the root is bracketed for the first time. A third-order polynomial is fitted and the root approximated by solving the cubic equation. In b., the function has been re-bracketed with the new root and a new polynomial fitted between the new brackets.

Table 1: Table of values used to define the “spine” of the distribution defining the second of the two synthetic test classes.

x	y
0.17	0.79
0.36	0.70
0.51	0.84
0.70	0.86
0.76	0.68
0.77	0.48
0.68	0.32
0.46	0.28
0.24	0.26

## 4 Comparison with competing algorithms using an artificial dataset

### 4.1 A pair of test classes

The AGF method was tested on a synthetic dataset consisting of the pair of classes shown in figure 3. The first class, illustrated using triangles, is a simple, two-dimensional normal distribution:

$$P(\vec{x}|1) = \frac{1}{2\pi\sigma_1\sigma_2} \exp \left\{ -\frac{1}{2} \left[ \left( \frac{x'}{\sigma_1} \right)^2 + \left( \frac{y'}{\sigma_2} \right)^2 \right] \right\} \quad (34)$$

$$\vec{x}' = \begin{bmatrix} \cos \theta & \sin \theta \\ -\sin \theta & \cos \theta \end{bmatrix} \cdot (\vec{x} - \vec{x}_0) \quad (35)$$

where  $\vec{x}_0$  is the centre of the distribution,  $\sigma_1$  and  $\sigma_2$  are the widths of its major and minor axes respectively,  $\theta$  is the angle of the major axis and  $\vec{x}' = (x', y')$ .

To produce a non-trivial interface between the two classes, the second one has a more intricate design. A set of points defining the “spine” of the distribution was chosen – see Table 1. Individual samples are first interpolated a random distance along the curve so defined using a cubic spline (Press *et al.*, 1992; Galassi *et al.*, 2007). By displacing this point a random distance in a random direction, the final location of the sample is determined.

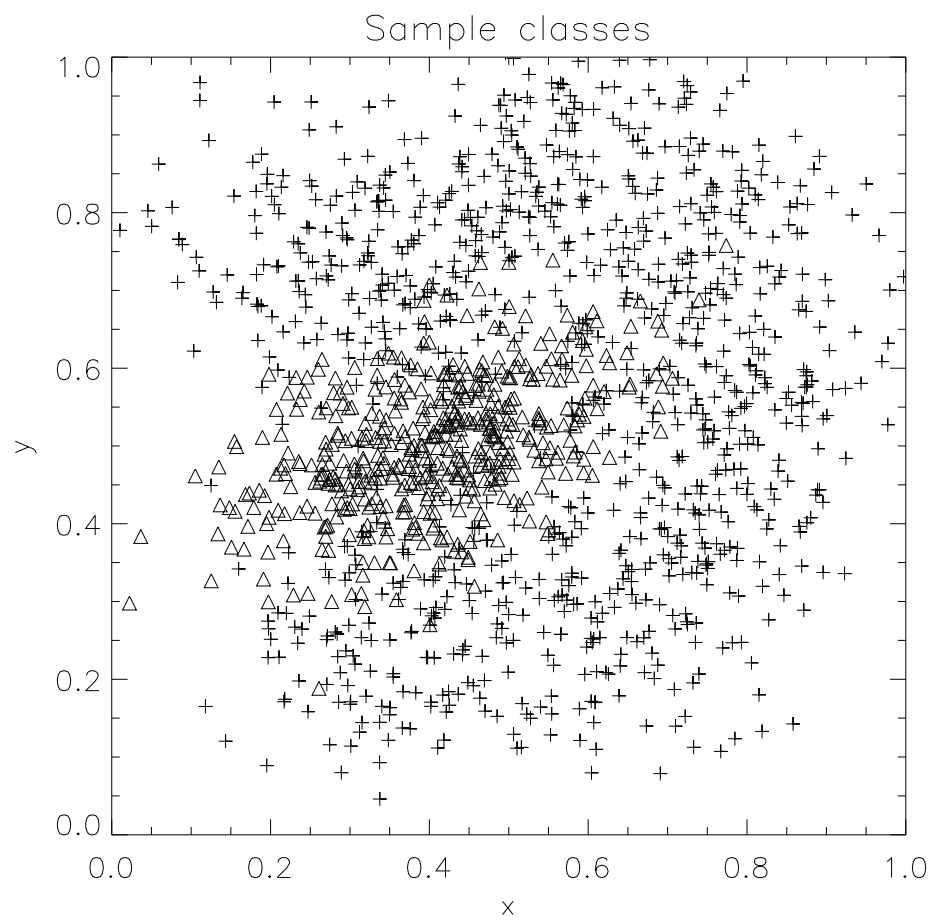


Figure 3: A pair of synthetic test classes

Analytic or semi-analytic (e.g. using numerical quadrature to perform the integration) values for the probability densities of the second class may be calculated as follows:

$$P(\vec{x}|2) = \frac{1}{s_{max}} \int_0^{s_{max}} Q(|\vec{x} - \vec{g}(s)|) ds \quad (36)$$

where  $\vec{g}$  is the line segment defining the spine,  $s$  is the path along it,  $s_{max}$  is its length and  $Q(r)$  is a circularly symmetric PDF governing the offset distance from the backbone. For the dataset shown in figure 3, a Gaussian (of width 0.1) was once again employed for  $Q$ .

## 4.2 Competing algorithms

To test the effectiveness of the AGF classification algorithm, it was compared with three other, popular methods. These are:  $k$ -nearest-neighbours (KNN), Learning Vector Quantisation (LVQ) and Support Vector Machines (SVM) and are briefly described below.

### 4.2.1 $K$ -nearest-neighbours

The KNN is one of the simplest and most robust classification methods available. It consists of finding the  $k$  training samples that are closest to the test point and then counting how many there are of each class. The class with the most samples is the class of the test point.

Our method reduces to a KNN by using a filter function that is one out to the filter width and zero everywhere else:

$$f(r) = \begin{cases} f(r) = 1, & r < \sigma \\ f(r) = 0, & r \geq \sigma \end{cases} \quad (37)$$

where  $\sigma$  is the filter width.

### 4.2.2 Learning Vector Quantisation

LVQ works by building up a set of “codebook vectors” whose density matches the difference between the densities of the two classes. The vectors will be labelled based on which class they fall within. The class of a test point will be given by the class label of the nearest codebook vector.

The training process is performed as follows: a set of codebook vectors are initialised at random points and assigned class labels. The codebook vectors are randomly compared with the training samples. If the labels of the two match, then the codebook vector is moved closer to the training sample. If they don't, then it is moved further away (Kohonen, 2000; Kohonen *et al.*, 1995).

### 4.2.3 Support Vector Machines

In SVM, a single hyperplane is drawn that best divides the two classes. Classifications are done as in equations (14)–(16) based on a dot product with the normal to the class border. The border is fitted by minimizing the classification error. Obviously, using a single straight line to divide the two synthetic sample classes will produce poor results. Results may be improved by adding variables derived from the originals thus expanding the dimension of the space, much as one fits a nonlinear function, e.g. a polynomial, by performing a linear fit on the set of variables formed by transforming the independent variables with a set of basis functions.

The so-called kernel trick can be applied to most algorithms that use scalar products and is based on the observation that certain mathematical operations applied to a scalar product will expand the variables in a set of basis functions, without having to explicitly calculate them. For example, consider the squared dot product of two two-dimensional variables (Müller *et al.*, 2001):

$$(\vec{x} \cdot \vec{y})^2 = [(x_1, x_2) \cdot (y_1, y_2)]^2 \quad (38)$$

$$= x_1^2 x_2^2 + 2x_1 y_1 x_2 y_2 + x_2^2 y_2^2 \quad (39)$$

$$= (x_1^2, \sqrt{2}x_1 x_2, x_2^2) \cdot (y_1^2, \sqrt{2}y_1 y_2, y_2^2) \quad (40)$$

## 4.3 Comparison results

Random synthetic datasets composed of 5000 samples of the first class and 10000 samples of the second class were created as needed using the algorithms described in section 4.1. Test datasets composed of three-thousand (3000) members were created separately and had no fixed ratio between the number of members in each class. Rather the ratio of the training data was used to randomly select which class was sampled.

Table 2: Comparison of parameters used in the KNN, LVQ, AGF and AGF borders classification algorithms

KNN	LVQ	AGF	AGF borders
$k = 101$	$\alpha_0 = 0.1$ $n_t = 75000$ $n = 1000$	$W_c = 100$ $k = 1000$	$W_c = 100$ $k = 1000$ $n = 250$ $\epsilon = 0.0001$

Table 3: Parameters used in the SVM classification algorithm

implementation:	LIBSVM
type:	C-SVC
kernel basis function:	$\exp(\gamma \vec{x}_i - \vec{x}_j ^2)$
$\gamma$ :	0.5
$C$ (cost):	100
$\epsilon$ :	0.001

The algorithm was also compared with an analytical classification scheme that compares the results of equations (34) and (36) applied to the test point. This has the advantage of quantifying the limit in accuracy of any classification algorithm, as well as returning the conditional probabilities.

Parameters for the KNN, LVQ, AGF and AGF borders techniques are compared in Table 2. For the LVQ method, Kohonen's so-called optimised LVQ 1 (OLVQ1) method was used.  $n_t$  is the number of training cycles, while  $n$  is the number of codebook vectors for the LVQ method and the number of border samples for the AGF border classification method. Note that AGF can be applied directly without searching for the class borders using equation (11). Also, performing the AGF classifications with all the data would be too slow, so the  $k$ -nearest-neighbours supplying the most weight are selected before applying the algorithm. This is done in  $n \log k$  time using a binary tree as described in section 3.2. The parameters used for the SVM method are listed in Table 3. The parameter  $\epsilon$  represents the fitting tolerance for both AGF and SVM. Parameters were hand-selected to maximize efficiency without compromising accuracy using the cross-validation procedure described above.



Table 4: Summary of validation and comparison results

Algorithm	training time (s)	classification time (s)	uncertainty coefficient	accuracy	correlation of R
Analytic	N/A	$1.29 \pm 0.20$	$0.53 \pm 0.02$	$0.906 \pm 0.005$	1.
KNN	N/A	$5.59 \pm 0.31$	$0.53 \pm 0.02$	$0.905 \pm 0.005$	$0.9953 \pm 0.0006$
AGF	N/A	$9.40 \pm 0.31$	$0.53 \pm 0.02$	$0.905 \pm 0.005$	$0.9979 \pm 0.0003$
AGF borders	$4.19 \pm 0.10$	$0.013 \pm 0.002$	$0.53 \pm 0.02$	$0.905 \pm 0.005$	$0.9972 \pm 0.0008$
LVQ	$2.81 \pm 0.01$	$0.101 \pm 0.003$	$0.50 \pm 0.02$	$0.898 \pm 0.006$	N/A
SVM	$112.4 \pm 3.6$	$2.22 \pm 0.15$	$0.53 \pm 0.02$	$0.905 \pm 0.005$	$0.9978 \pm 0.0003$

Table 4 shows the results of the comparison over twenty (20) trials. The uncertainty coefficient is a better method of validating classification results than simple accuracy (fraction of correct guesses) because it is not affected by the relative number of samples in each class. It is defined as follows:

$$H(i|j) = - \sum_{i,j} P(i,j) \ln P(i|j) \quad (41)$$

$$H(i) = \sum_i P(i) \ln P(i) \quad (42)$$

$$U(i|j) = \frac{H(i) - H(i|j)}{H(i)} \quad (43)$$

where  $i$  and  $j$  enumerate the true and retrieved classes respectively,  $P(i, j)$  is their joint probability,  $P(i|j) = P(i, j)/P(j)$  is their conditional probability, and  $P(i) = \sum_j P(i, j)$  is the total, invariant probability of the first class. If we think of the classification procedure as a noisy channel, then  $U(i|j)$  quantifies how many bits of knowledge we have of the true value of the class as a fraction of the maximum number of bits it is possible to transmit per classification (Press *et al.*, 1992; Shannon and Weaver, 1963).

The last column in the table is simply the correlation coefficient of the estimates of  $R(\vec{x})$  vs. the true values as computed by equations (34)–(36). For a visual comparison, see figures 4–7. Figure 8 compares estimates from AGF with borders training and without.

The main thing to note from this comparison is how much faster AGF with borders training is than the other four methods. This is important if

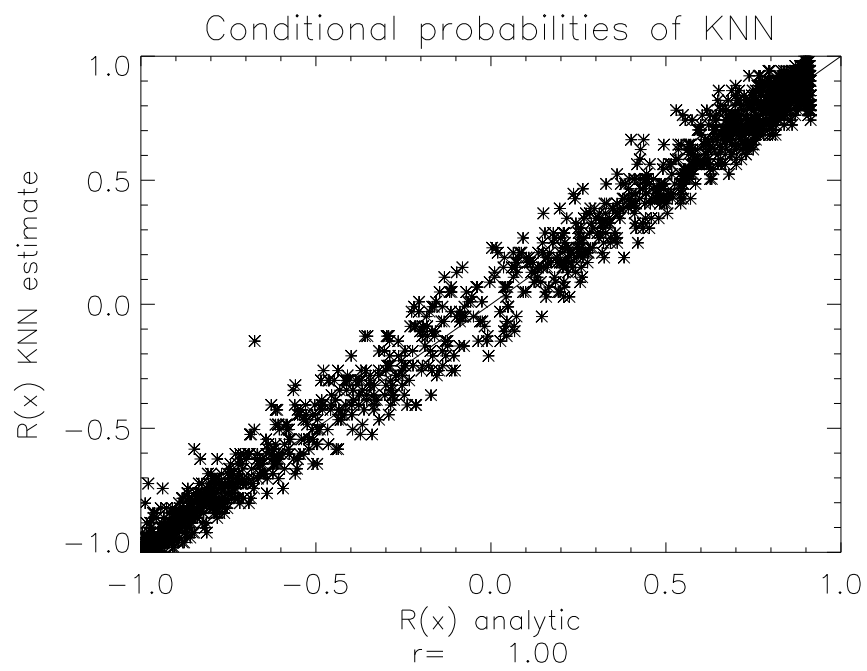


Figure 4: Comparison between estimates of conditional probabilities for the synthetic test classes. Y-axis is KNN, X-axis is semi-analytic.

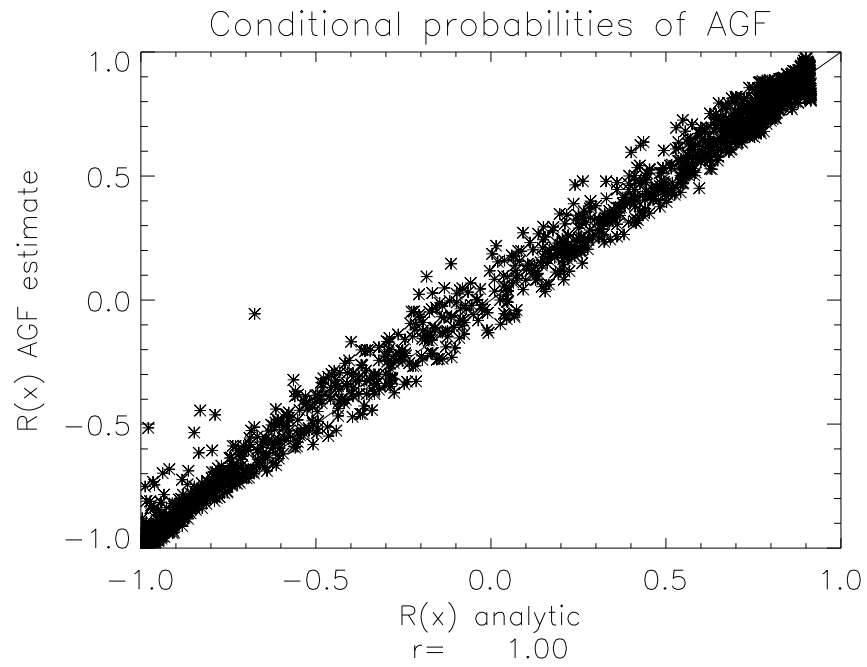


Figure 5: Comparison between estimates of conditional probabilities for the synthetic test classes. Y-axis is AGF without borders training, X-axis is semi-analytic.

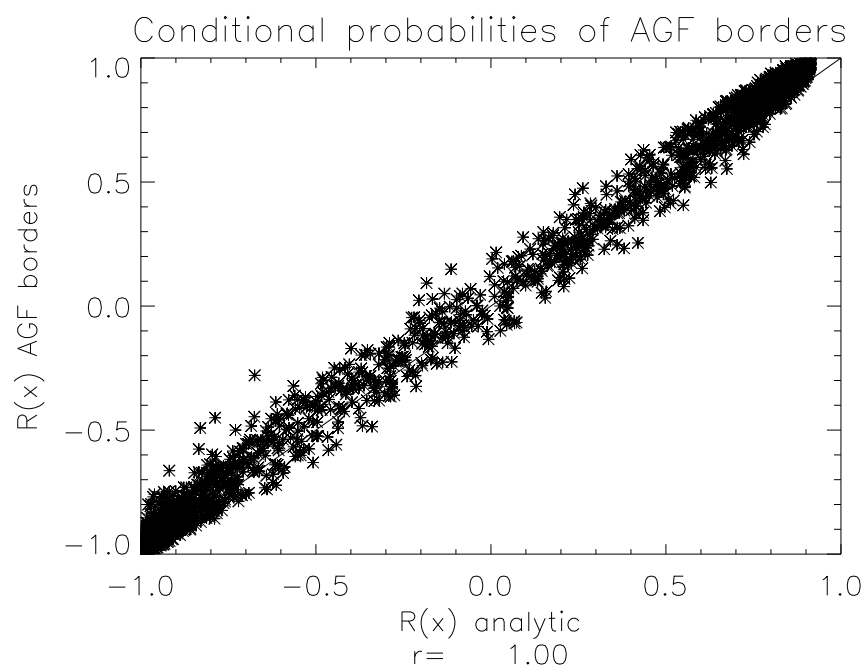


Figure 6: Comparison between estimates of conditional probabilities for the synthetic test classes. Y-axis is AGF with borders training, X-axis is semi-analytic.

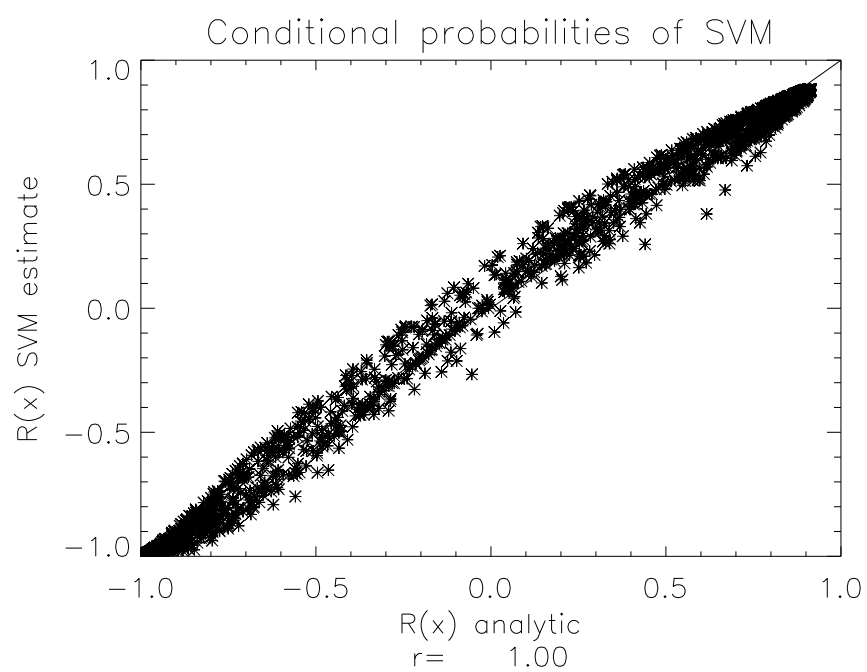


Figure 7: Comparison between estimates of conditional probabilities for the synthetic test classes. Y-axis is LIBSVM, X-axis is semi-analytic.

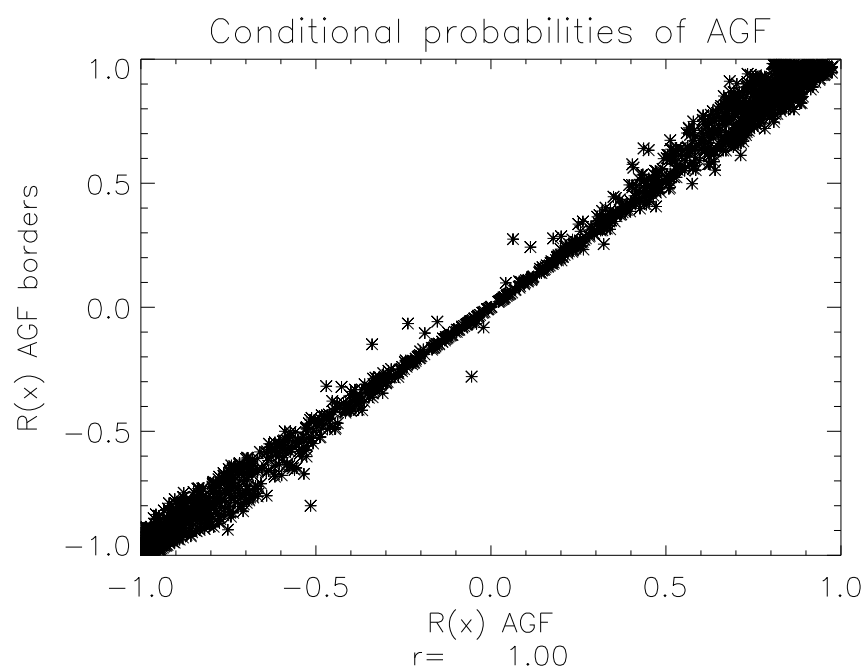


Figure 8: Comparison between estimates of conditional probabilities for the synthetic test classes. *Y*-axis is AGF with borders training, *X*-axis is AGF without.

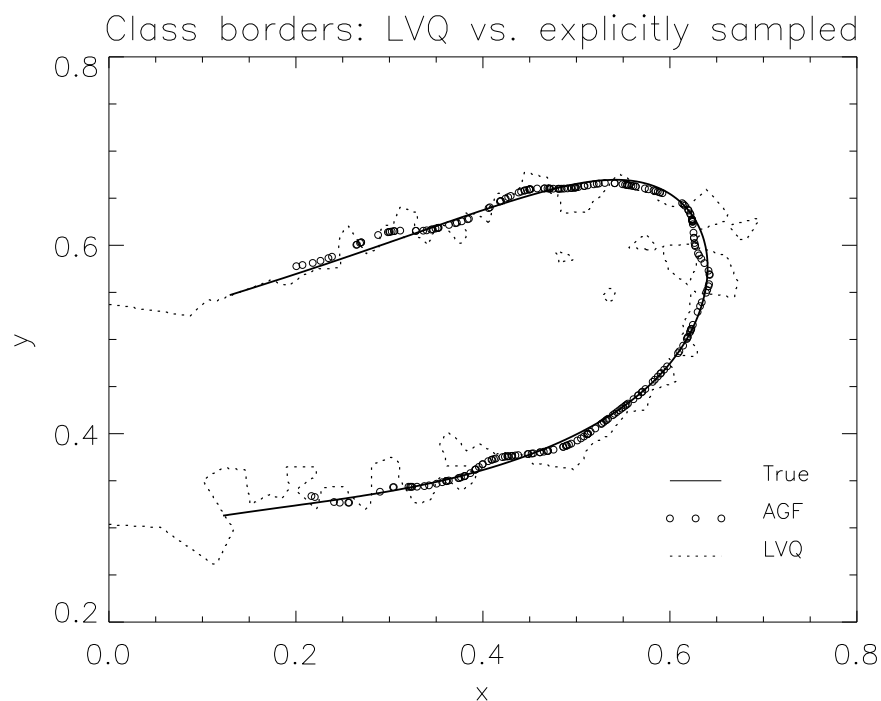


Figure 9: The class border of the synthetic test classes as characterized by three different methods.

we need to process large amounts of satellite data, especially in real time. The only other method that even comes close is LVQ, especially in the training phase, where it is much faster. Unfortunately, it does not supply any knowledge of the conditional probabilities, a necessary quantity for measuring the accuracy of a given classification with no prior knowledge of its true value. They are also useful for re-calibration of retrieved images, as will be demonstrated later.

Another short-coming of the LVQ method is that it samples very sparsely near the class borders, the exact region where we require the most knowledge. In fact the density of codebook vectors approaches zero at the class border; the method is actually designed this way! When we plot the class border between the codebook vectors from an LVQ training run, this produces a line that is jagged and meandering. Contrast this to the border found via AGF as shown in figure 4.3.

## 5 Application to Landsat images

Because of its global coverage and high resolution, Landsat 7 is one of the most sophisticated surface-mapping instruments. It images the globe using seven channels in the visible and near-infrared. Because of the 30 m resolution, any kind of processing will be highly computationally intensive. Landsat images are frequently used “as-is” to simulate aerial photographs by simply forming a colour image from three of the channels. A more powerful use, however, is feature-detection or surface classification using automated discrimination algorithms such as statistical classification.

The waterways in the Netherlands form a dense, complex network and because they produce dry land where once there was open sea are one of the engineering wonders of the world. Statistical classification was used to map the lakes, canals and rivers of the Netherlands based on a Landsat 7 image as seen in figure 10. Training data was selected manually from three images: two from Southern Ontario – LE70170292008280EDC00 and LE70180302008207EDC00 – whose surface is one third fresh water and one from Northern Germany – LE71960232008206ASN00 – whose landscape resembles the Netherlands. 1822 training samples were selected in total while the six Landsat 7 channels with 30 m resolution were used in the analysis.

Training times for AGF, LVQ, SVM and SVM with probability estimates were 0.5 s, 0.7 s, 0.15 s and 0.7 s, respectively. Classification times were 5.5 minutes, 20 minutes, 55 minutes and 58 minutes, respectively. In this example the training time is fairly immaterial because of the small number of samples, however for classification, AGF is nevertheless still the clear winner. 200 border samples were used. For LVQ, 200 “codebook” vectors were employed, although as implied in section 4.3, this is giving LVQ an unfair speed advantage since it will take more “codebook” vectors than border samples to represent the discrimination border to a similar level of precision.

Figure 11 demonstrates the utility of having the conditional probabilities available. Using a different set of lower-quality training data, many water points are now mis-classified as land. Therefore, we re-calibrate the algorithm by choosing a different, lower threshold value,  $R = -0.8$ , for the discrimination border, similar to what is described in Mills (2009). The corrected image is shown in figure 12. It is still not perfect, but the transformation has done a good job of re-classifying many of the points lying in the tidal flats as water instead of land.

In real-world problems, if the PDF’s of the classes are not monotonic



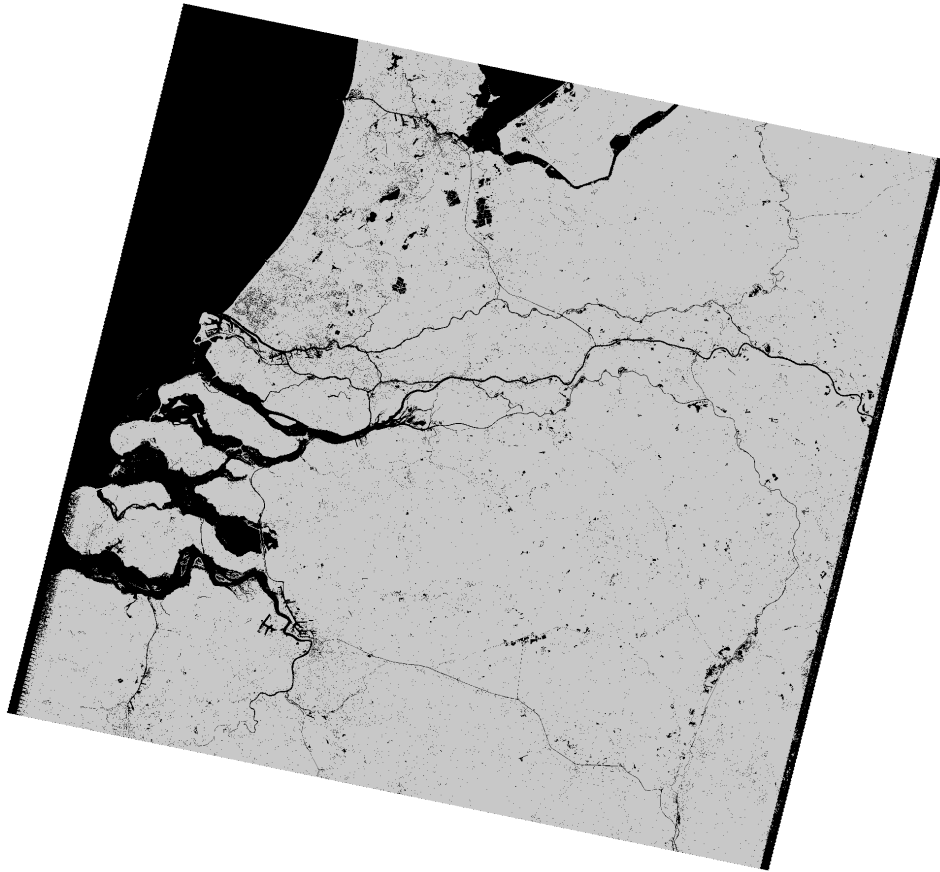


Figure 10: Landsat image (LE71980242002267EDC00) of the S. Netherlands whose pixels have been automatically classified into land and water using a training dataset derived from three other Landsat images.

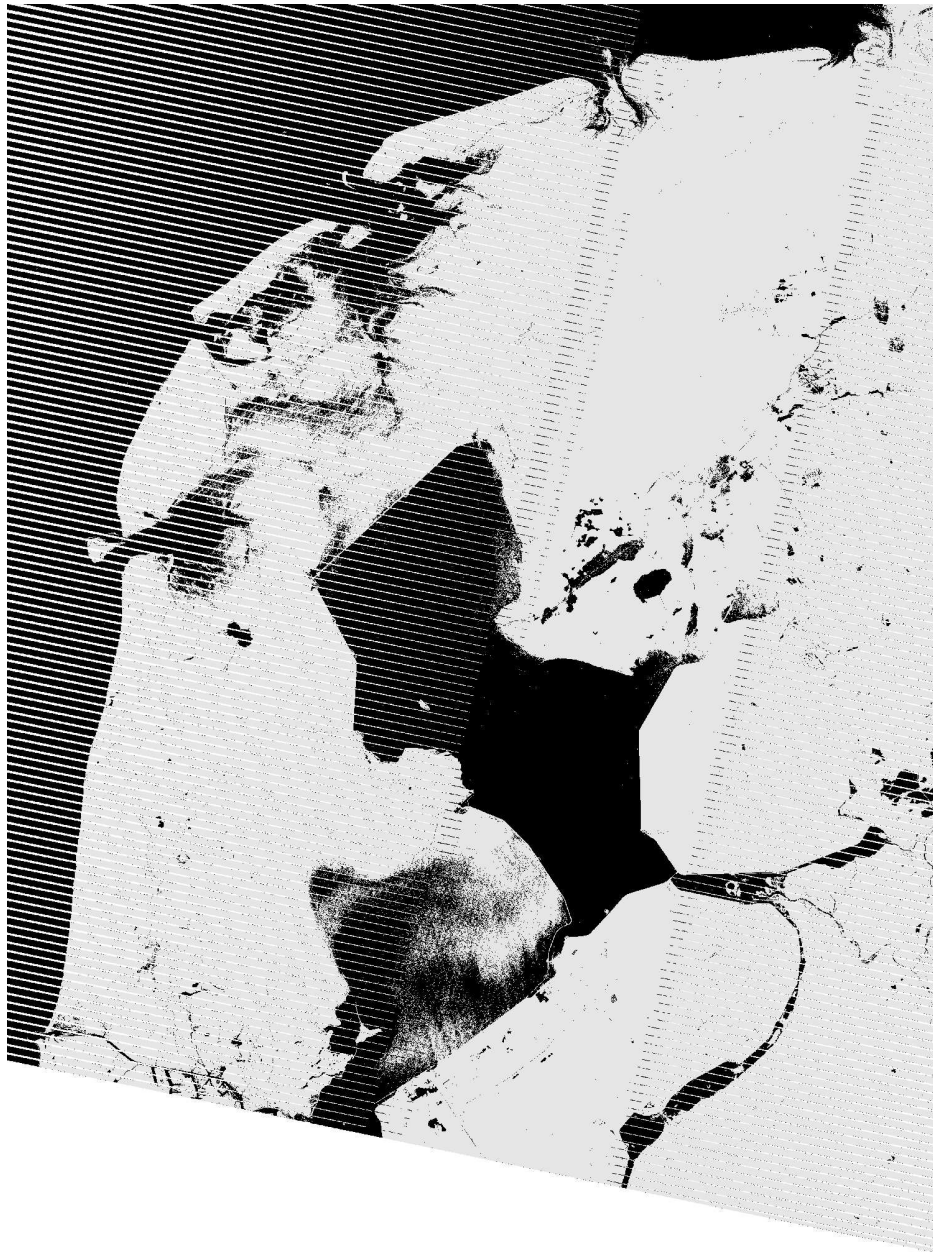


Figure 11: Landsat image (LE71980232007217ASN00) of the N. Netherlands whose pixels have been automatically classified into land and water. The horizontal striping is caused by a malfunction in the instrument control system affecting all Landsat 7 images after 31 May 2003.

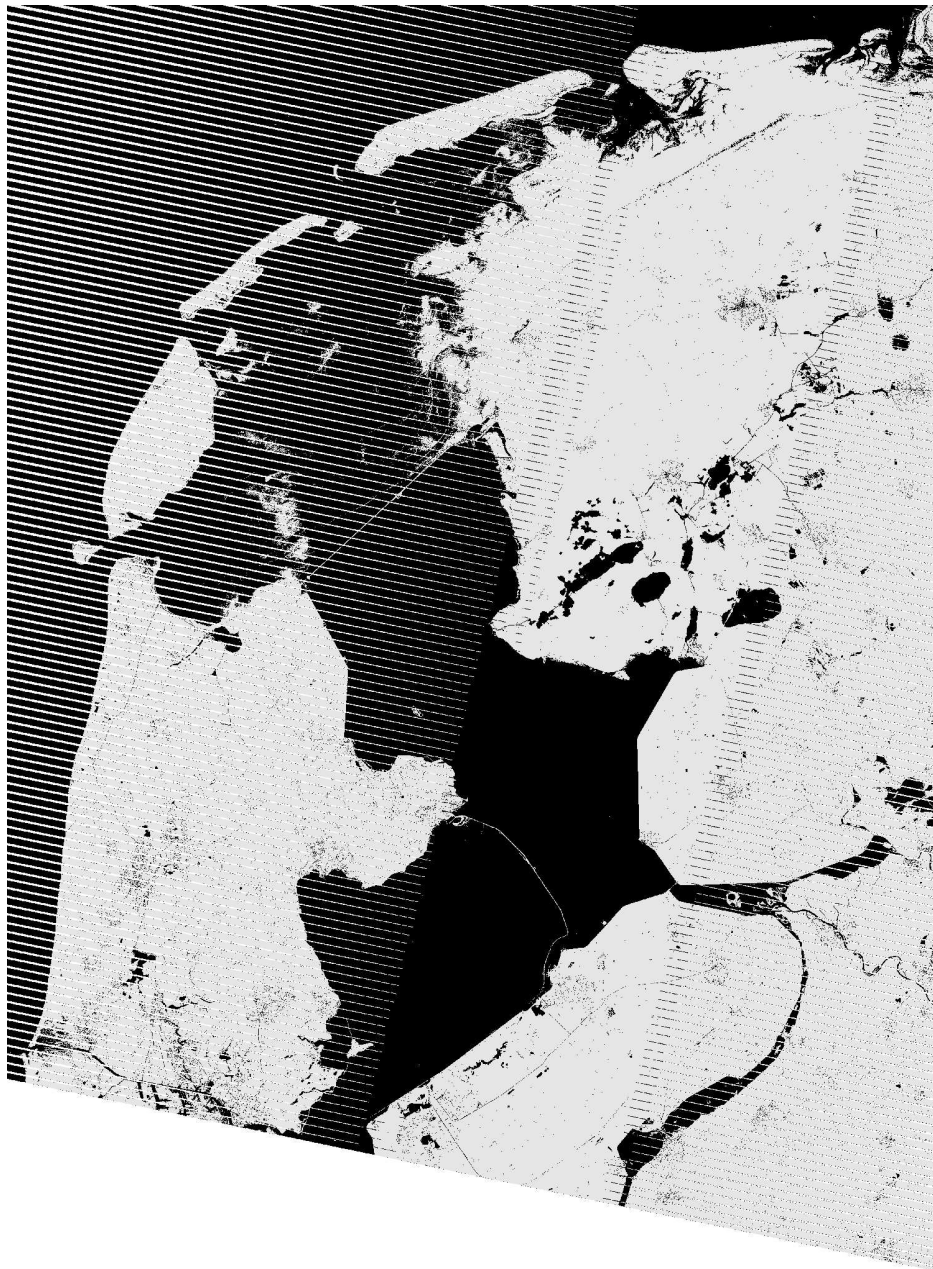


Figure 12: Landsat image (LE71980232007217ASN00) of the N. Netherlands whose pixels have been automatically classified into land and water. Image has been re-calibrated by shifting the discrimination border.

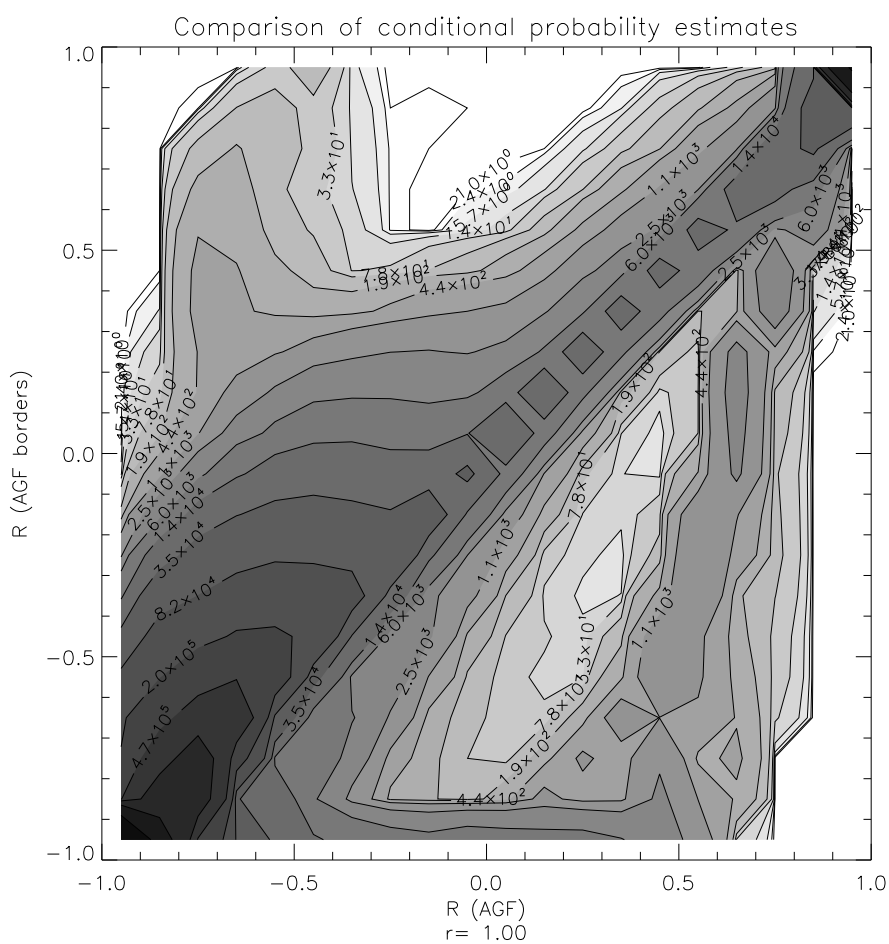


Figure 13: Comparison of conditional probability estimates using AGF with borders training versus direct AGF of pixels classified into land and water from Landsat 7 image LE71980242002267EDC00. Contours follow a geometric progression.



and roughly Gaussian near the borders, then conditional probability estimates based on (23) will be inaccurate. Fortunately, this is rarely the case. Figure 13 compares conditional probabilities estimated by extrapolation using equation (23) and more directly using the right-most side of equation (12) for the surface classifications illustrated in figure 10. In libSVM, conditional probabilities are also estimated using a one-dimensional parametrisation (Chang and Lin, 2001), so the best way to ensure accurate estimates is to apply one of the more direct methods – KNN or AGF without borders training.

## 6 Discussion

### 6.1 Algorithmic efficiency

The speed of the competing algorithms for a single problem does not tell the whole story since we also need to know the algorithmic efficiency, that is how the speed of the different algorithms depends on both the training set size and on the selection of parameters. In the case of KNN, classification times depend on the time it takes to select the  $k$  neighbours, in our case  $n \log k$  time. Since  $k$  is generally increased with increasing numbers of training samples, this means that the time dependence is more like  $n \log n$ . Actual tests of the selection algorithm, however, show a very weak dependence on  $k$ . Best case performance for a selection algorithm such as ours that sorts the results is actually  $n + k \log k$ , while for one that does not it is  $n$  (Knuth, 1998).

If this step is included, the bottleneck in the AGF algorithm is selecting the  $k$  nearest neighbours, hence the time efficiency will also be roughly  $n \log k$  worst case, although with further overhead of order  $k$  from calculating the weights. If the selection step is skipped, the time efficiency will be  $n$ , but with a large coefficient. Time efficiency for LVQ training will be  $n$ , while for SVM training, it is  $n^2$  since the solution of a matrix equation is required. Note that all methods will have extra overhead from reading in the training data and also from writing the output.

For algorithms that have a separate training phase, there is also the issue of the classification time. For both LVQ and AGF borders, classification times will be independent of the number of training samples. Time efficiency will rather depend linearly on the number of samples used to represent the discrimination border – codebook vectors for LVQ and border samples for

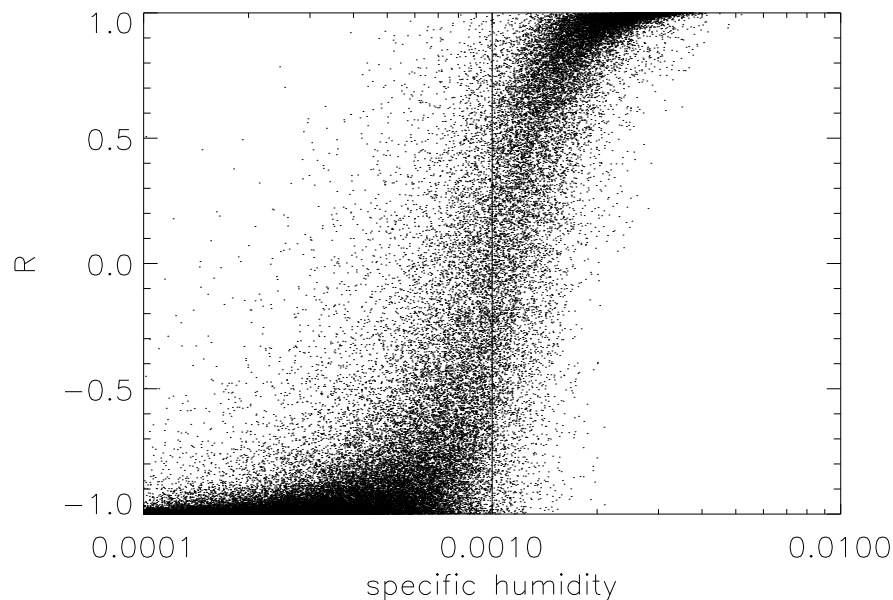


Figure 14: Comparison of conditional probability estimates with continuum values for a discrete water-vapour retrieval (threshold value for two ranges is set at 0.001 mass-mixing ratio). Conditional probabilities are estimated directly using AGF without borders training.

AGF – which are both adjustable parameters. The larger these parameters, the greater the accuracy, although with diminishing returns. For equivalent accuracy, more LVQ codebook vectors than AGF border samples will be needed.

In the case of SVM, classification times *do* depend on the number of training samples, which would seem to make the training phase a bit redundant. The time efficiency appears to be a bit better than  $n$ , where  $n$  is the number of training samples.

## 6.2 Use for continuum retrieval

Within the context of satellite remote sensing, statistical classification would appear to be a somewhat specialized tool, useful chiefly for processing images

by extracting features or classifying surface types. The method truly comes into its own, however, when recognised as an efficient, general, non-linear inverse method.

Like a neural network, statistical classification generates a direct inverse method that has the potential to be very fast. Unlike a neural network, however, there is no possibility of getting stuck in a local minimum when trying to optimise the model. Accuracy of the discrimination border is limited only by the resolution of the samples. The presence of local minima may also confound inverse methods, such as optimal estimation (Rodgers, 2000), that use a forward model directly.

Also unlike a neural network, statistical classification generates only discrete values: a limitation which is surprisingly easy to overcome. A continuum variable can be retrieved by dividing it into ranges. Designate the continuum variable as  $q$ . Just like in the discrete case, the relationship between the measurement variable,  $\vec{x}$ , and the state variable,  $q$ , will be governed by a conditional probability,  $P(q|\vec{x})$ . Suppose we divide  $q$  into two ranges with a threshold value,  $q_0$ , so that the classes are defined as follows:

$$c = \begin{cases} 1; & q < q_0 \\ 2; & q \geq q_0 \end{cases} \quad (44)$$

The continuum conditional probability is transformed to the discrete conditional probability by integration:

$$P(1|\vec{x}) = \int_{-\infty}^{q_0} P(q|\vec{x})dq \quad (45)$$

$$P(2|\vec{x}) = \int_{q_0}^{\infty} P(q|\vec{x})dq \quad (46)$$

If the divisions in  $q$  are made fine enough, i.e. smaller than the estimated error, then these can be used directly. Alternatively, the continuum value can be reconstituted in a number of other ways. For a two-dimensional retrieval, we can retrieve a series of isolines and then interpolate between them (Mills, 2009). If conditional probabilities are available, they can actually make quite a good proxy for the continuum result. Figure 14 compares conditional probabilities with continuum values from the water-vapour retrieval described in Mills (2009). It is easy to show from equations (45) and (46) that if the statistics of  $q$  for a given  $\vec{x}$  in  $P(q|\vec{x})$  are Gaussian, then the relationship

between the two will be an error function, as seen in the figure. Given:

$$P(q|\vec{x}) = \frac{1}{\sqrt{2\pi}\sigma_q} \exp \left\{ -\frac{[\bar{q}(\vec{x}) - q]^2}{2\sigma_q} \right\} \quad (47)$$

where  $\sigma_q$  is the width of the distribution and  $\bar{q}$  is the expectation value. Then:

$$R = \text{erf} \left[ \frac{\bar{q}(\vec{x}) - q_0}{\sqrt{2}\sigma_q} \right] \quad (48)$$

This result can be used not only to estimate the continuum result, but also to replace the hyperbolic tangent form used in equation (23) to estimate  $R$ . This assumes that  $\bar{q}$  is roughly linear in  $\vec{x}$  near the class border.

Another feature of such a retrieval is its robustness. Once classes have been defined, it is impossible to generate a result outside of this range. Moreover, it is easy to see from (45) and (46) that classification retrieval of continuum values is what is known as a robust estimator. Normally,  $q$  is estimated by evaluating its expectation value or first moment:

$$\bar{q} = \int_{-\infty}^{\infty} P(q|\vec{x})q dq \quad (49)$$

By contrast, the location of  $q_0$  is found by setting:

$$\int_{-\infty}^{q_0} P(q|\vec{x})dq = \int_{q_0}^{\infty} P(q|\vec{x})dq \quad (50)$$

or equalizing the fraction of “zeroth order” moment on each side of the threshold. This type of formulation is characteristic of robust estimators and results in outliers in the training data having less effect on the final model (Press *et al.*, 1992).

Finally, with the continuum variable divided into multiple ranges, returned error statistics can be made more detailed. By examining the conditional probabilities within each range, not only the statistics, but also the approximate functional form of the error may be determined.

## 7 Conclusion

A statistical classification algorithm based on kernel-density estimation was described, which we term Adaptive Gaussian Filtering or AGF. The many



refinements of this algorithm produce impressive speed gains compared to other methods making it appropriate for processing large amounts of satellite data, especially in real-time. As applied to a synthetic test dataset, the method is shown to be 25 times as fast for training and 125 times as fast for classification, when compared to LIBSVM, a Support Vector Machine implementation. The performance advantage becomes greater the larger the number of training samples. Therefore, when tested on real data, discriminating land from water in the Netherlands, the performance advantage was reduced because of the smaller training dataset – training times were roughly equivalent, while classification was ten times as fast.

The algorithm was also compared to  $k$ -nearest-neighbours (KNN) and Kohonen's Learning Vector Quantisation (LVQ). Three steps can be distinguished in the AGF algorithm. First, the conditional probabilities are estimated using kernel averaging. These estimates can be used directly to classify a set of test data from the training data, in a manner equivalent to a KNN. Second, the conditional probability estimates are used to search for the discrimination or class border in the case of a two-class classification. Once the discrimination border is known, it can be used to generate classification estimates more quickly than directly with the training data. Thus, KNN is not as fast as AGF when borders training is included.

While LVQ is similarly fast, both for training and classification, it does not return estimates of the conditional probabilities and is less accurate. Estimates of the conditional probabilities are useful for determining the accuracy of an estimate in absence of its true value. They are also useful for recalibrating an image when the classification estimates are biased.

Conditional probabilities are estimated using a simple parametrisation based on their gradients at the border. For the most accurate estimates of the conditional probabilities, a direct method such as KNN or AGF without borders training can be used. For most applications, however, the gains in accuracy will be too small to offset the significant speed penalty.

While statistical classification finds broad application in image processing techniques like feature extraction and surface detection, its full power as a general, non-linear inverse method has yet to be harnessed. Continuum variables can be retrieved by dividing them into discrete ranges. Such a technique has the advantage over a neural network or a more direct inverse method such as optimal estimation in that there is no possibility of becoming stuck in a local minimum. The accuracy of the estimates is limited only by the number and resolution of the training samples.

Software can be found at: <http://libagf.sourceforge.net>.

## Acknowledgements

Thank you very much to my colleagues from the IUP, University of Bremen for their continued support and encouragement of this work, in particular Stefan Buehler, Georg Heygster and Oliver Lemke. Thanks to Christian Melsheimer for his very valued comments on the draft manuscript.

This work was partially funded by the German Federal Ministry of Education and Research (BMBF), within the AFO2000 project UTH-MOS, grant 07ATC04. It is a contribution to COST Action 723 'Data Exploitation and Modeling for the Upper Troposphere and Lower Stratosphere'.

## References

- CHANG, C.C. and LIN, C.J., *LIBSVM: a library for support vector machines*. Software available at: <http://www.csie.ntu.edu.tw/~cjlin/libsvm>. 2001.
- GALASSI, M., DAVIES, J., THEILER, J., GOUGH, B., JUNGMAN, G., BOOTH, M. and ROSSI, F., *GNU Scientific Library: Reference Manual*. Available online at: <http://www.gnu.org/software/gsl>. 2007.
- KNUTH, D., 1998, *The Art of Computer Programming, Volume 3: Sorting and Searching*, 2nd edition (Addison-Wesley).
- KOHONEN, T., HYNINEN, J., KANGAS, J., LAAKSONEN, J. and TORKKOLA, K., 1995, LVQ PAK: The Learning Vector Quantization Package, Version 3.1. Technical report A30, Helsinki University of Technology, Laborator of Computer and Information Science. Available online at: <http://www.cis.hut.fi/research/som-research/nncr-programs.shtml>.
- KOHONEN, T., 2000, *Self-Organizing Maps*, 3rd edition (Springer-Verlag).
- LAUE, H., 2004, Automated Detection of Canola/Rapeseed from Space. PhD thesis, Institute of Environmental Physics, University of Bremen.
- MICHIE, D., SPIEGELHALTER, D.J. and TAYLER, C.C. (Eds) , 1994, *Machine Learning, Neural and Statistical Classification*, Ellis Horwood Series

in Artificial Intelligence (Upper Saddle River, NJ: Prentice Hall) (Available online at: <http://www.amsta.leeds.ac.uk/~charles/statlog/>).

MILLS, P., 2009, Isoline retrieval: An optimal method for validation of advected contours. *Computers & Geosciences*, **35**, pp. 2020–2031.

MÜLLER, K.R., MIKA, S., RÄTSCH, G., TSUDA, K. and SCHÖLKOPF, B., 2001, An Introduction to Kernel-Based Learning Algorithms. *IEEE Transactions on Neural Networks*, **12**, pp. 181–201.

PRESS, W.H., TEUKOLSKY, S.A., VETTERLING, W.T. and FLANNERY, B.P., 1992, *Numerical Recipes in C*, 2nd edition (Cambridge University Press).

RODGERS, C.D., 2000, *Inverse Methods for Atmospheric Sounding: Theory and Practice* (World Scientific).

SHANNON, C.E. and WEAVER, W., 1963, *The Mathematical Theory of Communication* (University of Illinois Press).

SPREEN, G., KALESCHKE, L. and HEYGSTER, G., 2008, Sea ice remote sensing using AMSR-E 89 GHz channels. *Journal of Geophysical Research*, **113** doi:10.1029/2005JC003384.

TERRELL, D.G. and SCOTT, D.W., 1992, Variable kernel density estimation. *Annals of Statistics*, **20**, pp. 1236–1265.

## A Gradient of an AGF estimate

2

Since the final result is just a summation of the filter weights, multiplied by some nominally constant values, we start by taking the gradients of the weights:

$$\frac{\partial w_i}{\partial x_j} = \left( \frac{\partial w_i}{\partial x_j} \right)_\sigma + \frac{\partial w_i}{\partial \sigma} \frac{\partial \sigma}{\partial x_j} \quad (51)$$

---

<sup>2</sup>This section does not appear in the original article.

Since the filter width is not constant, we must include a term to account for its change. The second factor of the second term, the gradient of the filter width, is not known, but we can easily solve for it by taking the derivative of the total weight, which is a constant:

$$\frac{\partial W}{\partial x_j} = \frac{\partial}{\partial x_j} \sum_i w_i \tag{52}$$

$$= \sum_i \frac{\partial w_i}{\partial x_j} \tag{53}$$

$$= \sum_i \left[ \left( \frac{\partial w_i}{\partial x_j} \right)_\sigma + \frac{\partial w_i}{\partial \sigma} \frac{\partial \sigma}{\partial x_j} \right] \tag{54}$$

$$= 0 \tag{55}$$

Solving:

$$\frac{\partial \sigma}{\partial x_j} = - \frac{\sum_i \left( \frac{\partial w_i}{\partial x_j} \right)_\sigma}{\sum_i \frac{\partial w_i}{\partial \sigma}} \tag{56}$$

For the case of a Gaussian filter the weights are given by:

$$w_i = \exp \left[ - \frac{d_i^2}{2\sigma^2} \right] \tag{57}$$

$$= \exp \left[ - \frac{\sum_j (x_{ij} - x_j)^2}{2\sigma^2} \right] \tag{58}$$

which generates the following partials:

$$\left( \frac{\partial w_i}{\partial x_j} \right)_\sigma = \frac{(x_{ij} - x_j)}{\sigma^2} w_i \tag{59}$$

$$\frac{\partial w_i}{\partial \sigma} = \frac{d_i^2}{\sigma^3} w_i \tag{60}$$

Substituting these into equations (56) and (51) respectively, produces the following:

$$\frac{\partial \sigma}{\partial x_j} = -\frac{\sigma \sum_i (x_{ij} - x_j) w_i}{\sum_i d_i^2 w_i} \quad (61)$$

$$\frac{\partial w_i}{\partial x_j} = \frac{w_i}{\sigma^2} \left[ x_{ij} - x_j - d_i^2 \frac{\sum_k (x_{kj} - x_j) w_k}{\sum_k d_k^2 w_k} \right] \quad (62)$$

For a two class classification, the gradient of the difference of the conditional probabilities is given as follows:

$$\frac{\partial R}{\partial x_j} \approx \frac{1}{W} \sum_i \frac{\partial w_i}{\partial x_j} (2c_i - 3) \quad (63)$$

$$\approx \frac{1}{W\sigma^2} \sum_i w_i (2c_i - 3) \left[ x_{ij} - x_j - d_i^2 \frac{\sum_k (x_{kj} - x_j) w_k}{\sum_k d_k^2 w_k} \right] \quad (64)$$

using our rather awkward convention of enumerating the first class by “1” and the second by “2.”